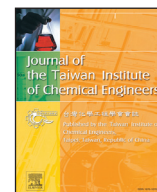




Contents lists available at ScienceDirect

Journal of the Taiwan Institute of Chemical Engineers

journal homepage: [www.elsevier.com/locate/jtice](http://www.elsevier.com/locate/jtice)

# Fabrication of bismuth molybdate photocatalyst co-substituted by gadolinium and tungsten for bismuth and molybdenum: Design and radical regulating by the synergistic effect of redox centers and oxygen vacancies for boosting photocatalytic activity

Hongda Li, Wenjun Li\*, Xintong Liu, Chaojun Ren, Fangzhi Wang, Xiao Miao

Beijing Key Laboratory for Science and Application of Functional Molecular and Crystalline Materials, University of Science and Technology Beijing, Xueyuan Road No. 30, Haidian District, Beijing 100083, China

## ARTICLE INFO

### Article history:

Received 23 January 2018

Revised 10 April 2018

Accepted 12 April 2018

Available online xxx

### Keywords:

Gd/W co-substituted bismuth molybdate

Photocatalysis

Redox center

Oxygen vacancy

## ABSTRACT

Substitutive doping is a fundamental approach to introduce dopants into a crystalline structure, which resulted in generating the abundant redox centers or oxygen vacancies to promote the separation of photogenerated charge carriers. However, the recombination rate of electron-hole pairs in the single-substituted photocatalysts remained high, thus co-substituting of two sites could be further synergistically restraining the recombination of electron-hole pairs. Herein, the bismuth molybdate ( $\text{Bi}_2\text{MoO}_6$ ) photocatalyst, co-substituted by  $\text{Gd}^{3+}$  and  $\text{W}^{6+}$  ions for  $\text{Bi}^{3+}$  and  $\text{Mo}^{6+}$  ions, was synthesized using a hydrothermal method. X-ray photoelectron spectra indicated that the abundant oxygen vacancies were generated in the crystalline  $\text{Bi}_2\text{MoO}_6$  after introducing  $\text{W}^{6+}$  ions, and these vacancies adsorbed the extensive  $\text{O}_2$  molecules. Additionally, the results of photoluminescence spectra, photocurrent response and trapping experiments demonstrated that the new hydroxyl radicals can be generated by introducing  $\text{Gd}^{3+}$  ions, while the introducing of  $\text{W}^{6+}$  ions contributed to enhancing the productivity of  $\bullet\text{O}_2^-$  radicals; these two species together promoted the separation and transfer of electron-hole pairs. The results of photocatalytic experiments displayed that Gd/W co-substituted  $\text{Bi}_2\text{MoO}_6$  shows much better visible-light photocatalytic activity. These findings developed a novel synergistic effect between redox centers (Gd substitution) and oxygen vacancies (W substitution) to design the high-efficiency photocatalysts.

© 2018 Taiwan Institute of Chemical Engineers. Published by Elsevier B.V. All rights reserved.

## 1. Introduction

In the past decades, semiconductor photocatalytic technique has been a green and beneficial approach for the water splitting,  $\text{CO}_2$  reduction, organic pollutants decomposition and so on [1–6]. Undoubtedly, the semiconductor photocatalyst of  $\text{TiO}_2$  has been extensively studied due to its efficient photocatalytic performance, high physical and chemical stability, as well as low cost and nontoxicity [7,8]. However, more and more the visible-light photocatalysts have been developed and studied because  $\text{TiO}_2$  has only a response to ultraviolet light that covers only 3–5% of solar spectra. These visible-light-driven photocatalysts mainly include metal sulfide (such as  $\text{ZnS}$  and  $\text{CdS}$ ) [9,10], metal oxide (such as  $\text{Fe}_2\text{O}_3$ ,  $\text{WO}_3$  and Zn-Fe-layered metal hydroxides) [11–13], oxyhalide (such as  $\text{BiOCl}$  and  $\text{BiOBr}$ ) [14,15], and  $\text{A}_x\text{B}_y\text{O}_z$  (A and B = metal elements). Among these visible-light photocatalysts,

the studies about the  $\text{A}_x\text{B}_y\text{O}_z$  visible-light photocatalysts covered the largest quantity, such as  $\text{BaTiO}_3$ ,  $\text{Ag}_2\text{MoO}_4$ ,  $\text{LiInO}_2$ ,  $\text{Bi}_2\text{MoO}_6$ , and so on [16–19]. However, the applications of the pure  $\text{A}_x\text{B}_y\text{O}_z$  photocatalysts have been limited by the high recombination ratio of photogenerated charge carriers or the limited visible-light absorption. In order to resolve these difficulties, fabrication of modified materials by doping of metal or non-metal ions [20,21], building heterojunction or homojunction structure [22,23], and loading noble-metal co-catalysts [24,25] have been widely studied. These results of the modified photocatalysts demonstrated that the separation of charge carriers could be available promoted, or the visible light absorption can be extended to longer wavelengths.

Doping is a simple and controllable approach to introduce dopants into a crystalline structure, which could lead to generating the redox centers or crystal defects (usually the oxygen vacancies in the crystal of  $\text{A}_x\text{B}_y\text{O}_z$ ) [26–28]. Both the oxygen vacancies and redox centers could control the separation process of charge carriers, which contributed to adjusting the properties of semiconductor photocatalysts. Huang reported that the formed

\* Corresponding author.

E-mail address: [wjli\\_ustb@163.com](mailto:wjli_ustb@163.com) (W. Li).

surface oxygen vacancies played a role in the trapping centers for photo-generated electrons, thus facilitating the separation of photo-generated charge carriers and the production of dominant reactive species hydroxyl radicals for photodegrading MO [29]. From our previous studies, ions-doping could introduce the abundant redox centers to tremendously promote the separation and transfer of charge carriers and result in the enhanced photocatalytic activity [26,30]. For the substitutive doping of  $A_xB_yO_z$  photocatalysts, the results of the A-site substitution might lead to the production of the various lattice defects or redox centers [31,32]. These products are conductive to enhance the separation efficiency of electron-hole pairs or extended light absorption, and then resulted in improved photocatalytic activity. For the O-site, it is usually doping of some non-metal elements (such as N and B elements) [33,34], contributing to enhancing the photoelectric property through introducing the doping level or oxygen vacancies. Similarly, the substitution of B-site may induce a little modification of crystal structure to generate abundant lattice defects because of the different ionic radius, resulting in noticeable effect on the mobility of electron-hole pairs and photocatalytic property [35]. However, the recombination efficiency of photo-generated charge carriers in the single-substituted  $A_xB_yO_z$  photocatalysts remained high, thus co-substituting of two sites in  $A_xB_yO_z$  is a potential stratagem for further synergistically restraining the recombination of electron-hole pairs. Also, there are just some studies about A-site/O-site and B-site/O-site co-substituted  $A_xB_yO_z$  to synergistically enhance the photocatalytic activity, such as Sm/N co-doped  $Bi_2WO_6$  and W/N co-doped  $NaTaO_3$  [36,37]; while the development of the new synergistic effect by A-site and B-site co-substituting could be also an available approach to improve the photocatalytic performance, and it has seldom been reported for all we know.

In this work, bismuth molybdate ( $Bi_2MoO_6$ ), as a typical and greatly popular  $A_xB_yO_z$  visible-light photocatalyst, was chosen as host material [38]. Meanwhile,  $Gd^{3+}$  was chosen as a dopant to substitute the  $Bi^{3+}$  (A-site); because the doping of  $Gd^{3+}$  ions could introduce redox centers into the lattice and contribute to generating the  $\cdot OH$  radicals from our previous studies [39], and the Gd-doped photocatalysts displayed the high-efficiency photocatalytic activity [40,41]. Then,  $W^{6+}$  ion was selected to substitute the  $Mo^{6+}$  ion (B-site), which profited from their similar ionic radius and same oxidation state [42]; and the small difference in ionic radius could be conductive to form oxygen vacancies. In this way, a novel Gd/W co-substituted  $Bi_2MoO_6$  photocatalyst was prepared by using a hydrothermal method for the first time. The results of photodegradation experiments demonstrated that Gd/W co-substituted  $Bi_2MoO_6$  displayed apparently improved photocatalytic activity compared with pure  $Bi_2MoO_6$  or single-substituted  $Bi_2MoO_6$ . The mechanism about the influences of Gd/W elements co-substitution on the photocatalytic activity of  $Bi_2MoO_6$  photocatalyst was also systematically studied.

## 2. Experimental section

### 2.1. Preparation of pure $Bi_2MoO_6$ (pure BMO), Gd-substituted $Bi_2MoO_6$ (Gd-BMO), W-substituted $Bi_2MoO_6$ (W-BMO), and Gd/W co-substituted $Bi_2MoO_6$ (Gd/W-BMO)

The pure and ions-substituted BMO photocatalysts were prepared using a facile hydrothermal approach.  $Bi(NO_3)_3 \cdot 5H_2O$  (2 mmol) and  $(NH_4)_6Mo_7O_{24} \cdot 4H_2O$  (0.14 mmol) were dissolved in 40 mL of 2 mol  $L^{-1}$  nitric acid solution and 30 mL of Milli-Q water to be the clear solutions, respectively. Ammonium molybdate solution was then added into the bismuth nitrate solution, and the mixture was stirred for 20 min. Subsequently, a different amounts of the gadolinium nitrate or sodium tungstate solutions were added into the above mixtures, respectively; the pH values

of systems were adjusted to about nine with the dilute  $NH_3 \cdot H_2O$  solution. After 20 min of stir, the obtained precursors were placed in a 100 mL Teflon-lined stainless autoclave. The autoclaves were heated to 180 °C and maintained for 12 h. In the end, the precipitates were filtered and washed with Milli-Q water three times, and then were dried at 80 °C for several hours. The obtained photocatalysts were as listed below: pure BMO, 1.0% Gd-BMO (1Gd-BMO), 2.0% Gd-BMO (2Gd-BMO), 5.0% Gd-BMO (5Gd-BMO), 2.0% Gd/0.5% W-BMO (2Gd/0.5W-BMO), 2.0% Gd/1.0% W-BMO (2Gd/1W-BMO), 2.0% Gd/2.0% W-BMO (2Gd/2W-BMO), and 1.0% W-BMO (1W-BMO).

### 2.2. Characterization of catalysts

The crystalline phases of the obtained catalysts were recorded using X-ray diffraction (XRD; D/MAX-RB, Rigaku, Japan) in the  $2\theta = 10^\circ\text{--}70^\circ$  range with a Cu  $K\alpha$  source ( $\lambda = 0.15405$ ). The morphologies differences of the catalysts were examined using a scanning electron microscope (SEM; SU8010, Hitachi, Japan) operated at 15.0 kV and transmission electron microscope (TEM; F-20, FEI, USA) at accelerating voltage of 200 kV. X-ray photoelectron spectra (XPS) were performed on an X-ray photoelectron spectrometer (EscaLab 250Xi, Thermo, USA) with an Al  $K\alpha$  source. The UV-vis diffuse reflectance spectra (DRS) of samples were collected by an UV-vis spectrophotometer (T9s, Persee, China) with  $BaSO_4$  as a reference. The photoluminescence (PL) spectra were measured by a fluorescence spectrophotometer (F-4500, Hitachi, Japan) with a xenon lamp as excitation light source. Photo-electrochemical measurement was collected by an electrochemical workstation (5060F, RST, China) with a conventional three-electrode system.

### 2.3. Photocatalytic activity tests

The photocatalytic activities of the Degussa P25 (~80% anatase and ~20% rutile) and as-prepared samples were respectively estimated by the photodegradation of rhodamine B (RhB, 12 mg  $L^{-1}$ ), phenol (30 mg  $L^{-1}$ ), and methylene blue (MB, 10 mg  $L^{-1}$ ) using a 400 W xenon lamp irradiation with a 420 nm cut off filter. In each experiment, the 30 mg sample was uniformly scattered in 30 mL organic solution. Prior to irradiation, the suspensions were vigorously stirred for 60 min in the darkness to reach an adsorption-desorption equilibrium. During the photoreaction, about 3 mL the uniform distribution of suspensions were respectively taken out per 5 min for RhB degradation, 1 h for phenol degradation, and 40 min for MB degradation; then, centrifuged to remove the solid samples. The concentrations of the RhB, phenol or MB were respectively analyzed by the absorbance at 553, 270 or 664 nm using a T9s spectrophotometer.

## 3. Results and discussion

### 3.1. Material structures, morphologies and chemical states analysis

The crystalline structure of the obtained samples was determined by X-ray diffraction (XRD). Fig. 1 reveals that all the XRD patterns of pure BMO and ions-substituted BMO perfectly coincided with a koechlinite phase of  $Bi_2MoO_6$  (JCPDS card no. 21-0102), though the Gd or W elements were added in the process of synthesis. Also the introducing of Gd or W elements did not generate any new phases due to their low concentration [43]. Apparently, the peak intensities of the substituted samples decreased compared with pure BMO, which attributed to the weakened degree of cationic ordering through substituting by gadolinium or tungsten. These results also implied that the partial  $Bi^{3+}$  ions (103 pm) and  $Mo^{6+}$  ions (65 pm) have been successfully substituted by the  $Gd^{3+}$  ions (94 pm) and  $W^{6+}$  ions (62 pm) in the lattice

Download English Version:

<https://daneshyari.com/en/article/7104528>

Download Persian Version:

<https://daneshyari.com/article/7104528>

[Daneshyari.com](https://daneshyari.com)